JOURNAL OF VIROLOGY, July 1997, p. 5277–5286 Vol. 71, No. 7
0022-538X/97/$04.00+0

Hemagglutinin-Esterase, a Novel Structural Protein of Torovirus

LISETTE A. H. M. CORNELISSEN,[1,2] CHRISTEL M. H. WIERDA,[1] FREEK J. VAN DER MEER,[1] ARNOLD A. P. M. HERREWEGH,[1] MARIAN C. HORZINEK,[1] HERMAN F. EGBERINK,[1] AND RAOUL J. DE GROOT[1]*

Virology Unit, Department of Infectious Diseases and Immunology,[1] and Department of Large Animal Medicine and Nutrition, Veterinary Faculty,[2] Utrecht University, 3584 CL Utrecht, The Netherlands

Received 4 November 1996/Accepted 18 March 1997

We have characterized the 3′-most 3 kb of the genome of bovine torovirus (BoTV) strain Breda. A novel 1.2-kb gene, located between the genes for the membrane and nucleocapsid proteins, was identified. This gene, the 3′-most 0.5 kb of which is also present in the genome of the equine torovirus isolate Berne virus (BEV), codes for a class I membrane protein displaying 30% sequence identity with the hemagglutinin-esterases (HEs) of coronaviruses and influenza C viruses. Heterologous expression of the BoTV HE gene yielded a 65,000-molecular weight N-glycosylated protein displaying acetylesterase activity. Serologic evidence indicates that the HE homolog is expressed during the natural infection and represents a prominent antigen. By using an antiserum raised against residues 13 to 130 of HE, the HE protein was detected in radioiodinated, sucrose gradient-purified BoTV preparations. Formal evidence that HE is a structural protein was provided by immunoelectron microscopy. In addition to the large, 17- to 20-nm spikes, BoTV virions possess shorter surface projections (6 nm on average). We postulate that these surface projections, which are absent from the BEV virion, are composed of the BoTV HE homolog. The HE gene, which has now been demonstrated in three different virus genera, is a showpiece example of modular evolution.

RNA viruses are genetically very flexible. During the replication of their genomes, nucleotide substitutions occur at a high frequency, allowing swift adaptation to selective pressure. For some viruses, homologous RNA recombination, i.e., genetic exchange between closely related RNA molecules, functions as a correction mechanism counteracting genetic drift and Muller's ratchet (7). At the same time, it allows the rapid horizontal spread of advantageous mutations (for a review on RNA recombination, see reference 34). Heterologous RNA recombination involves nonrelated RNA molecules and provides a means to acquire blocks, or modules, of new genetic information either from other viruses or from the host (18, 54, 69).

One of the most remarkable examples of heterologous recombination is that of the coronavirus hemagglutinin-esterase (HE) gene. Coronaviruses are enveloped, positive-stranded RNA viruses with a genome of about 30 kb in length. Some coronavirus species possess, in addition to the spike (S), membrane (M), envelope (E), and nucleocapsid (N) proteins, a fifth structural protein, HE (for a review, see reference 1). This 65-kDa class I membrane protein has 30% amino acid identity with the HE-1 subunit of the HE fusion protein (HEF) of influenza C virus (ICV), a negative-stranded RNA virus with a segmented genome (1, 36). It has been speculated that coronaviruses have captured the HE module from ICV or a related virus during a mixed infection (36). Presumably, this event occurred after coronavirus speciation, since the HE gene is present only in the genomes of viruses related to mouse hepatitis virus and is absent in the antigenic coronavirus clusters represented by feline infectious peritonitis virus and infectious bronchitis virus (35). Both in ICV and in coronaviruses, HE displays an acetylesterase activity specific for *N*-acetyl-9-*O*-acetylneuraminic acid (21–23, 28, 58, 59). The ICV HEF serves as a receptor-binding and receptor-destroying protein (21, 58), and it has been argued that the coronavirus HE has similar functions (44, 60).

Surprisingly, HE-like sequences have been found in the genome of yet another virus, the torovirus Berne virus (BEV) (48). Toroviruses, which are enveloped positive-stranded RNA viruses of cattle, pigs, horses, and possibly humans, form a separate genus in the *Coronaviridae* family (for a review, see reference 51). Their genomic organization and replication strategy closely resemble those of coronaviruses. However, the spike and membrane proteins of toro- and coronaviruses, though similar in size and structure, do not have evident sequence identity (11, 49). Also, there are striking differences in nucleocapsid morphology (15, 64). Hence, toro- and coronaviruses are related but are separated by a considerable evolutionary distance.

BEV, an equine isolate, is the only torovirus that can be grown in tissue culture, and it is therefore the best studied. The 3′-most 15 kb of its 25- to 30-kb genome has been sequenced, identifying the genes for Pol 1b, S, M, and N (51). In addition, a nonfunctional open reading frame (ORF), ORF4, was found. Translation of this ORF yielded a polypeptide sequence 30% identical to the C-terminal 142 amino acids of the HE(−1) proteins of ICV and coronavirus (48). These findings have led to the hypothesis that the HE gene may be part of the standard gene repertoire of torovirus and that BEV is a mutant that has lost part of its HE gene during tissue culture adaptation (48). Here we present the first genetic characterization of bovine torovirus (BoTV) strain Breda 2, a torovirus field isolate antigenically closely related to BEV (31, 67, 68). Evidence is provided that (i) BoTV carries an intact, functional gene for an HE homolog and (ii) the torovirus HE is a structural protein. The implications of our findings for virus evolution and the possible origin of the HE module are discussed.

* Corresponding author. Phone: 31-30-2532460. Fax: 31-30-2536723. E-mail: R.Groot@vetmic.dgk.ruu.nl.

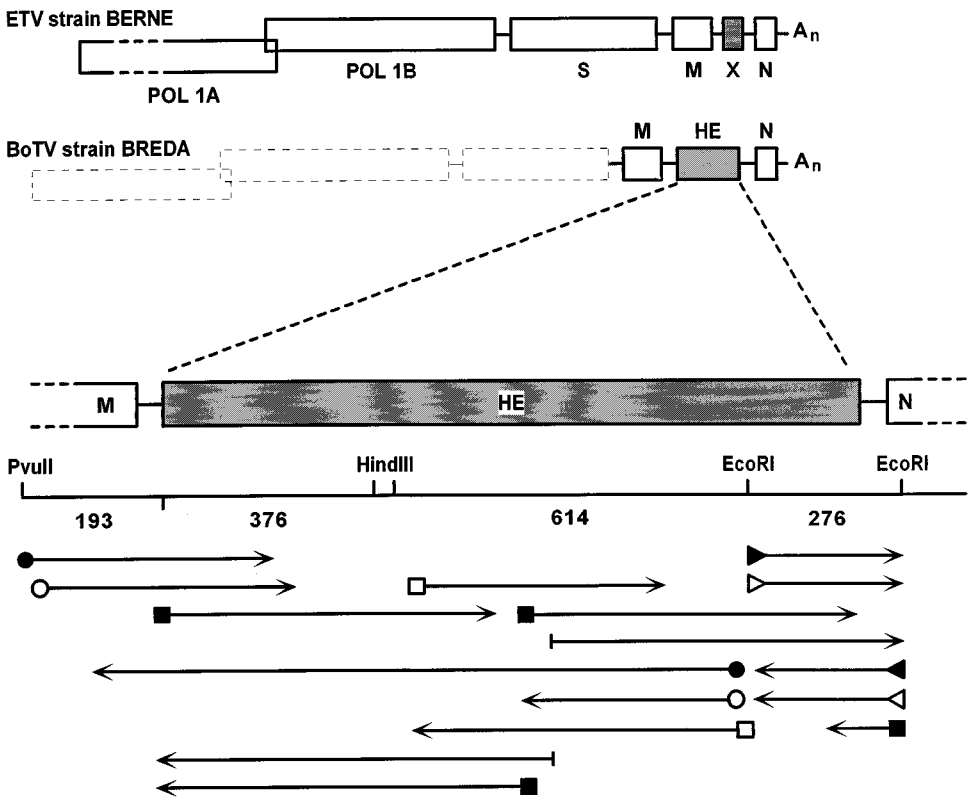

FIG. 1. Schematic outline of the strategy used for the cDNA cloning and sequence analysis of the BoTV HE gene. The upper part shows the genomic organizations of the equine torovirus (ETV) isolate Berne and BoTV strain Breda 2. The genes for the polymerase polyproteins (POL 1A and POL 1B) and for the structural proteins S, M, and N are indicated. Also indicated, by shaded boxes, are the genes for the HE homolog of BoTV and the HE-related BEV pseudogene (X). The lower part depicts the sequencing strategy for the BoTV HE gene. Different symbols represent independent cDNA clones. The clone indicated with (I) was used in the vTF7-3 expression studies.

MATERIALS AND METHODS

Cells, viruses, and antisera. BHK-21 cells and OST7-1 cells (14) were maintained in Dulbecco's modified Eagle's medium (DMEM) supplemented with 10% heat-inactivated fetal calf serum (FCS), 100 IU of penicillin per ml, and 100 μg of streptomycin per ml (DMEM–10% FCS). Recombinant vaccinia virus vTF7-3 expressing the bacteriophage T7 RNA polymerase gene (16) was provided by B. Moss. BoTV strain Breda 2 and antisera from gnotobiotic calves infected with BoTV strain Breda 2 (GC76) or bovine coronavirus (GC78) were obtained from G. Woode (32, 68). The rabbit antisera against BEV and BoTV strain Breda 2 were described previously (29, 30). W4461 is a field serum from a BoTV-infected cow, as identified in a BEV-neutralizing assay (10).

Isolation and reverse transcription-PCR (RT-PCR) amplification of genomic RNA of BoTV strain Breda 2. To isolate genomic RNA, sucrose gradient-purified BoTV (30) was mixed with an equal volume of TES buffer (20 mM Tris [pH 7.4], 1 mM EDTA, 100 mM NaCl) containing 2% sodium dodecyl sulfate (SDS) and 7 M urea and incubated for 5 min at room temperature. The RNA was extracted with phenol-ether and ethanol precipitated. Oligonucleotide primer 294 (5′-CT TACATGGAGACACTCAACCA-3′), designed on the basis of sequences from the 3′ noncoding region of the BEV genome (50), was used for the synthesis of first-strand cDNA as described by Herrewegh et al. (19). The cDNA was amplified by PCR by using oligonucleotides designed on the basis of sequences from the BoTV N gene (oligonucleotide 375) and the BEV M gene (oligonucleotide 376). PCR was performed for 35 cycles (1 min at 94°C, 1 min at 55°C, and 2 min at 72°C) in a final reaction volume of 100 μl containing 5 μl of the cDNA reaction mixture, 0.2 μM each primer, 200 μM deoxynucleoside triphosphates, 2 mM $MgCl_2$, 1× PCR buffer (Pharmacia), and 2 U of *Taq* DNA polymerase. The resulting 1.6-kb PCR product was purified from a 1% low-melting-point agarose gel (FMC Bioproducts); digested with *Pvu*II, *Eco*RI, and *Hin*dIII; and subcloned into pUC20 (Boehringer Mannheim). The expression plasmid, pBS-HE, containing the BoTV gene under the control of the bacteriophage T7 promoter, was constructed as follows. PCR was performed with primers 388 and 375, using first-strand cDNA generated with primer 294 as a template. The resulting 1.3-kb PCR product was inserted into *Eco*RV-digested pBluescript K/S+ (Stratagene).

Nucleotide sequence analysis. Sequence analysis was performed by using the T7 DNA polymerase sequencing kit according to the instructions of the manufacturer (Pharmacia Biochemicals). The nucleotide sequence was determined for both orientations by using two or more independent clones (Fig. 1). The oligonucleotide primers used for cloning and sequence analysis are listed in Table I. Nucleotide and amino acid sequences were analyzed by using the PC-DOS HIBIO DNASIS and PROSIS software from Pharmacia Biochemicals.

Transfection of vTF7-3-infected OST7-1 cells with pBS-HE and metabolic labeling. Subconfluent monolayers of OST7-1 cells grown in 35-mm-diameter dishes were infected with vTF7-3 at a multiplicity of infection of 10 at 37°C. At 1 h postinfection (p.i.), the cells were transfected with plasmid pBS-HE. For this purpose, the inoculum was replaced by a mixture of 0.5 ml DMEM, 10 μl of Lipofectin (GIBCO BRL, Life Technologies, Inc.), and 2.5 μg of plasmid DNA. After a 5-min incubation at room temperature, an additional 0.5 ml of DMEM was added, and incubation was continued at 37°C. The incubation temperature was lowered to 32°C at 2 h p.i. From 4.5 to 5 h p.i., the cells were incubated with 1 ml of minimal essential medium lacking cysteine and methionine (GIBCO BRL, Life Technologies, Inc.); 70 μCi of ^{35}S-in vitro labeling mix (Amersham) was then added to the culture medium, and the incubation was continued for various times. The cells were harvested either immediately or after a chase with DMEM–10% FCS containing 2 mM (each) L-methionine and L-cysteine.

RIPA. Metabolically labeled cells were washed once with ice-cold phosphate-buffered saline (PBS) and lysed on ice in 600 μl of lysis buffer (20 mM Tris-HCl [pH 7.5], 1 mM EDTA, 100 mM NaCl, 1% Triton X-100, 1 mM phenylmethylsulfonyl fluoride). When indicated, 20 mM *N*-ethylmaleimide (NEM) (Sigma) was added to both washing and lysis buffers to prevent the formation of nonnative disulfide bonds (9). Nuclei and cell debris were pelleted for 4 min at 10,000 × *g* at 4°C. One hundred microliters of the supernatant was mixed with 1 ml of detergent solution (50 mM Tris-HCl [pH 8], 62.5 mM EDTA, 0.4% Na-deoxycholate, 1% Nonidet P-40), SDS was added to a final concentration of 0.25%, and the mixture was incubated for 10 min on ice. Subsequently, 2 μl of antiserum was added, and the mixtures were incubated for 16 h at 4°C. To collect the immune complexes, 15 μl of a 10% (wt/vol) suspension of formalin-fixed *Staphylococcus aureus* cells (Pansorbin; Calbiochem) was added. After a 30-min incubation at 4°C, the immune complexes were washed three times with radioimmunoprecipitation assay (RIPA) buffer (10 mM Tris-HCl [pH 7.5], 150 mM NaCl, 0.1% SDS, 1% Na-deoxycholate, 1% Nonidet P-40) and suspended in 25

TABLE 1. Oligonucleotide primers used for RT-PCR and sequence analysis

Primer	Nucleotide sequence (5′ to 3′)	Orientation	Position[a]
253	GAGAAAGAGCCAAGATGAATT[b]	Sense	1286–1306
375	GAAAAACCTGATGGGTACTGCAT	Antisense	1366–1388
376	GAACAGGAAGTTTTGCAATTGC[c]	Sense	(−)346–(−)325
386	CTGTGGTGTTGCATCATAATACC	Antisense	683–705
387	CACACACCAGCTTGTAGTGTTGGC	Antisense	444–467
388	CCACTTATCTAGAGAAGATGCTG	Sense	(−)17–6
389	GGAACCAGGCACTTATAATGCATC	Sense	753–776
402	GCGGCAACACCAGTAACACCATAT	Sense	40–63
422	GGACGAGGATGACTTTGATG	Antisense	182–201
427	ATGGATCCTTTGCGGCAACACCAGTA	Sense	29–54
428	TAGAATTCCATTTGATAAAGCTTAGT	Antisense	373–398
489	CATCAAAGTCATCCTCGTCC	Sense	182–201
613	ATGATGCAGGGTCTTTTGAGGAAT	Sense	1006–1029

[a] Position counted from the start codon of the HE gene.
[b] Designed on the basis of sequences from the BEV N gene (50).
[c] Sequence derived from the M gene of BEV (11).

μl of Laemmli sample buffer either immediately or after treatment with endoglycosidase H (EndoH) (Boehringer Mannheim) as described by Machamer et al. (37). The samples were heated for 5 min at 95°C and analyzed in SDS-polyacrylamide gels.

Indirect immunofluorescence. Subconfluent monolayers of BHK-21 cells grown on 12-mm-diameter gelatin-coated coverslips were infected with vTF7-3 and transfected with plasmid pBS-HE as described above. At 6 h p.i., the cells were fixed with 3% paraformaldehyde and either permeabilized with PBS containing 1% Triton X-100 or left untreated. Immunofluorescence was performed as described by Opstelten et al. (43). The cells were incubated for 1 h with the rabbit antiserum against BoTV, diluted 1:100 in PBS–50 mM glycine, washed, and then stained for 30 min with fluorescein isothiocyanate-conjugated goat anti-rabbit immunoglobulin G (diluted 1:200) (Cappel). The cells were embedded in Fluorsave (Calbiochem) and examined with an Olympus BH2-RFCA microscope.

In situ acetylesterase assay. Subconfluent monolayers of BHK-21 cells grown on 12-mm-diameter gelatin-coated coverslips were infected with vTF7-3 and transfected with pBS-HE as described above. At 6 h p.i., the cells were fixed with ice-cold formalin-acetone. Acetylesterase activity was detected as described by Wagaman et al. (63) with α-naphthylacetate-pararosanilin as a substrate. The cells were examined by phase-contrast microscopy.

Preparation of monospecific rabbit antiserum against BoTV HE. To prepare an antiserum against HE, nucleotide residues 35 to 391 were PCR amplified with oligonucleotide primers 427 and 428 and pBS-HE DNA as a template. The PCR product was cut with *Bam*HI and *Eco*RI and inserted into pGEX-2T (Pharmacia Biotech). The resulting construct was used to express amino acid residues 13 to 130 of HE as a glutathione *S*-transferase (GST) fusion protein in *Escherichia coli* PC2495 (47). The expression product was purified from SDS-polyacrylamide gels as described previously (33) and used for immunization of a New Zealand White rabbit as described by Chirnside et al. (8).

Electron microscopy. Formvar-carbon-coated copper grids were placed on 5-μl drops of sucrose gradient-purified BoTV and left for 1 h. Immunoelectron microscopy was performed as described by Vennema et al. (57) with the rabbit anti-HE serum diluted 1:100 in PBS, containing 0.5% bovine serum albumin (BSA) (fraction 5; Sigma) and 1% acetylated BSA (BSA-C; Aurion), and a protein A–5-nm colloidal gold conjugate. For negative controls, grids with BoTV were incubated with either rabbit preimmune serum or a rabbit antiserum against a fusion protein consisting of GST and amino acid residues 255 to 328 of feline herpesvirus gE (39). The grids were examined with a Philips CM10 electron microscope.

RESULTS

Identification of an HE gene in the genome of bovine torovirus. Sucrose-gradient purified BoTV strain Breda, prepared from the feces of an experimentally infected gnotobiotic calf (30, 68), was used as a source of viral RNA. This RNA served as a template for RT-PCR with BEV sequence-derived oligonucleotides (Table 1). Amplified cDNA, together covering the 3′-most 3 kb of the BoTV genome, was cloned into pGEM-T vectors and sequenced. The strategy for cDNA cloning and sequence analysis is outlined in Fig. 1.

Three ORFs were found, the 5′- and 3′-most of which were identified as the genes for the membrane protein M and the nucleocapsid protein N, respectively (details will be reported elsewhere). The third ORF, 1,248 nucleotides in length, codes for a polypeptide of 416 residues with the characteristics of a class I glycoprotein. Computer analysis of the amino acid sequence predicted a cleavable N-terminal signal sequence of 14 residues (Fig. 2). Residues 393 to 415 form a potential transmembrane domain. The presumptive ectodomain contains 17 cysteine residues, which may be involved in disulfide bond formation, and seven potential N-linked glycosylation sites. Remarkably, the presumptive cytoplasmic domain consists of only a single cysteine residue (Fig. 2).

Only the 3′-most 426 nucleotides of this ORF are present as a pseudogene in the BEV genome; Snijder et al. (48) previously noted that the deduced amino acid sequence of this gene remnant shows a striking similarity to the HE-1 subunit of ICV and the HE protein of coronaviruses (36). Our present data suggest that BoTV contains an intact gene for an HE homolog. The BoTV HE homolog is about 30% identical to the HE-1 subunit of ICV and the HE protein of coronavirus. The ICV and coronavirus HE proteins show a similar degree of sequence similarity (36). An amino acid sequence alignment of these proteins is shown in Fig. 3. The F-G-D-S motif, identified as the putative catalytically active site of the acetylesterases of ICV and coronaviruses (22, 61), is also conserved in the BoTV HE homolog.

The torovirus HE protein is a 65K protein that is expressed during BoTV infection of cattle. The BoTV HE homolog was studied biochemically by using the vaccinia virus vTF7-3 expression system (16). vTF7-3-infected OST7-1 cells were transfected with pBS-HE, a pBluescript vector carrying the HE gene under the control of the T7 promoter, and metabolically labeled for 30 min with [^{35}S]Met-Cys. Mock-transfected cells served as a negative control. Cell lysates were subjected to RIPA with a rabbit antiserum raised against sucrose gradient-purified BoTV. Upon analysis of the immunoprecipitates in reducing SDS-polyacrylamide gels, a product with an M_r of 65,000 (65K) was detected in pBS-HE-transfected but not in mock-transfected cells (Fig. 4a). The 65K product was not precipitated by rabbit preimmune serum or by a rabbit antiserum raised against BEV. These results identified the 65K product as the BoTV HE protein. The HE protein was also precipitated by convalescent-phase serum of a BoTV-inoculated gnotobiotic calf and by sera from naturally infected cattle (Fig. 4b), indicating that the torovirus HE gene is functional and expressed during the natural infection.

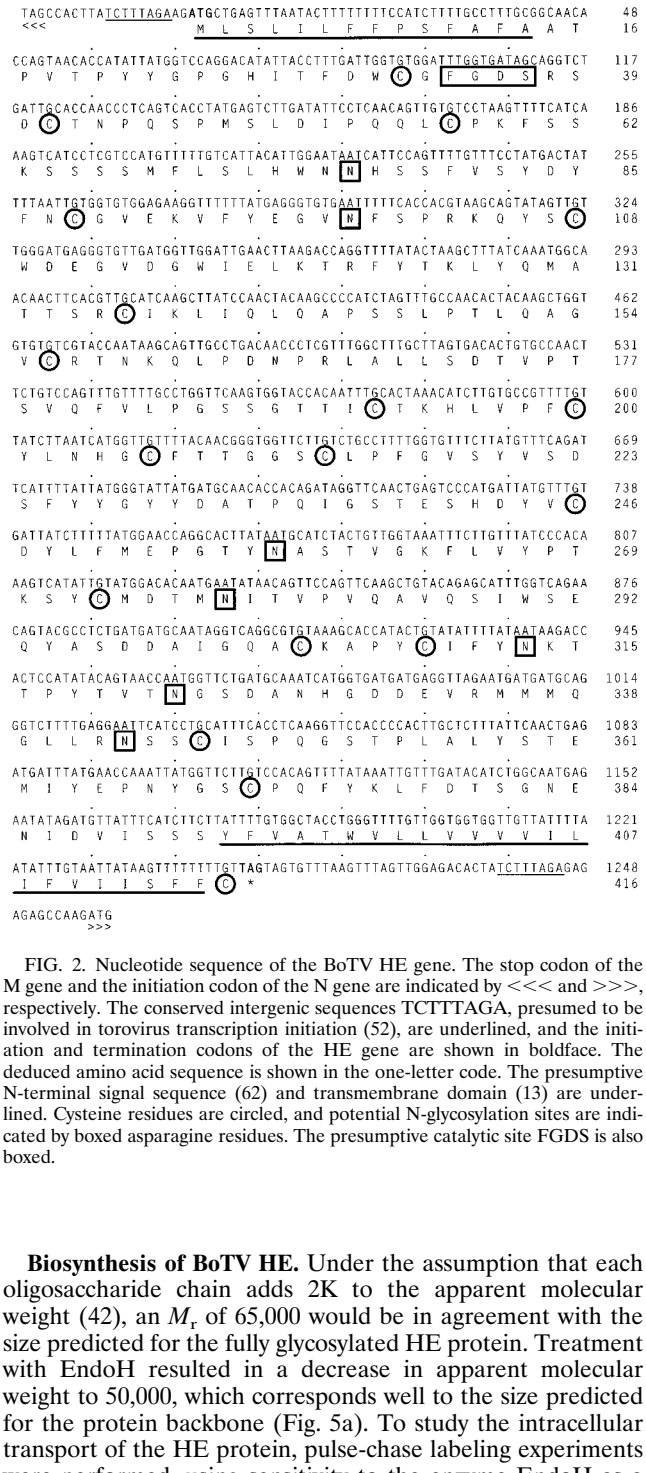

FIG. 2. Nucleotide sequence of the BoTV HE gene. The stop codon of the M gene and the initiation codon of the N gene are indicated by <<< and >>>, respectively. The conserved intergenic sequences TCTTTAGA, presumed to be involved in torovirus transcription initiation (52), are underlined, and the initiation and termination codons of the HE gene are shown in boldface. The deduced amino acid sequence is shown in the one-letter code. The presumptive N-terminal signal sequence (62) and transmembrane domain (13) are underlined. Cysteine residues are circled, and potential N-glycosylation sites are indicated by boxed asparagine residues. The presumptive catalytic site FGDS is also boxed.

Biosynthesis of BoTV HE. Under the assumption that each oligosaccharide chain adds 2K to the apparent molecular weight (42), an M_r of 65,000 would be in agreement with the size predicted for the fully glycosylated HE protein. Treatment with EndoH resulted in a decrease in apparent molecular weight to 50,000, which corresponds well to the size predicted for the protein backbone (Fig. 5a). To study the intracellular transport of the HE protein, pulse-chase labeling experiments were performed, using sensitivity to the enzyme EndoH as a biochemical assay. As shown in Fig. 5a, HE was transported, albeit inefficiently, from the endoplasmic reticulum (ER) to the medial Golgi compartments, where conversion to EndoH resistance occurs. These results were confirmed by immunofluorescence microscopy. HE produced predominantly a reticular cytoplasmic staining but was also observed in a distinct perinuclear compartment, reminiscent of the Golgi complex, and on the cell surface (Fig. 6a).

The HEF of ICV assembles into noncovalently associated homotrimers, whereas coronavirus HE forms disulfide-linked

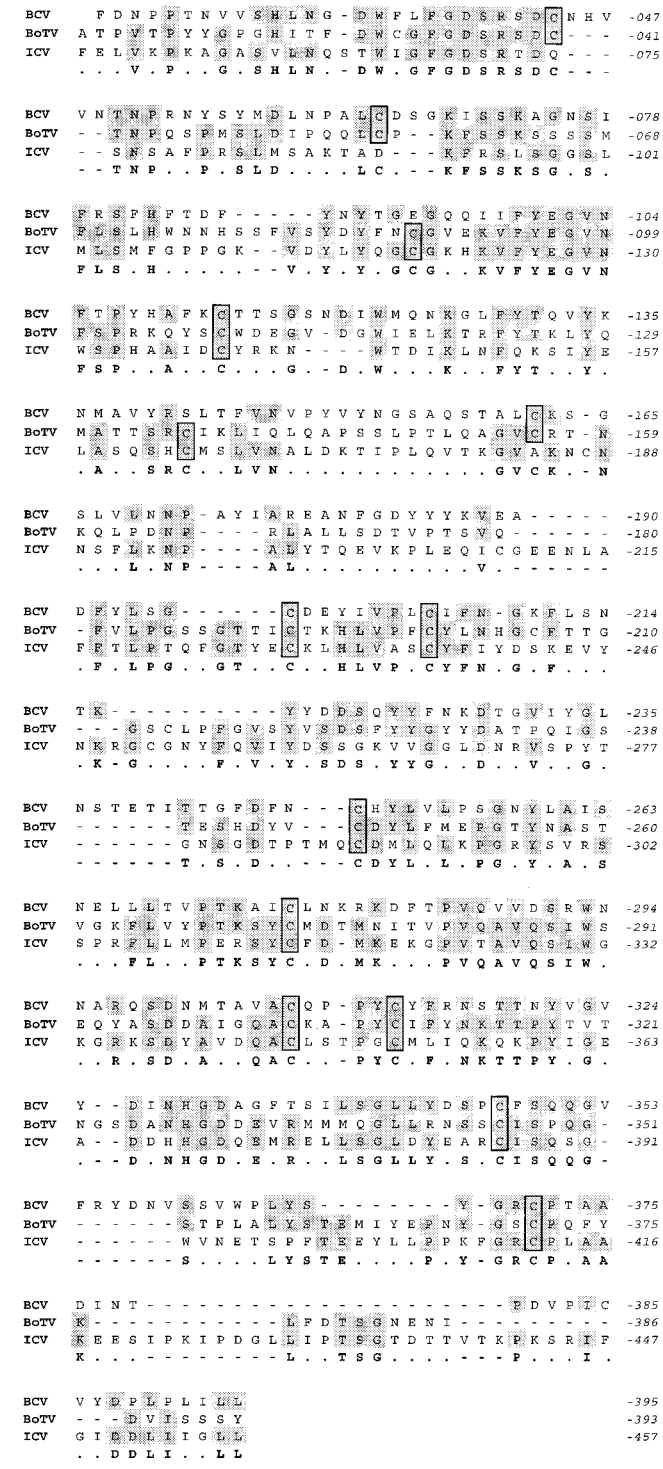

FIG. 3. Alignment of the amino acid sequences of the bovine coronavirus strain Mebus HE (26), the HE-1 subunit of ICV strain C/Cal/78 (41), and the HE of BoTV strain Breda 2. Conserved amino acid residues are indicated by shading, and conserved cysteine residues are boxed. The consensus sequence is shown in boldface, with dots representing nonconserved residues.

homodimers (12, 24, 25). To determine whether torovirus HE forms disulfide-linked oligomeric complexes, pBS-HE-transfected, vTF7-3-infected cells were lysed in the presence of NEM to block free sulfhydryl groups (9), and immunoprecipi-

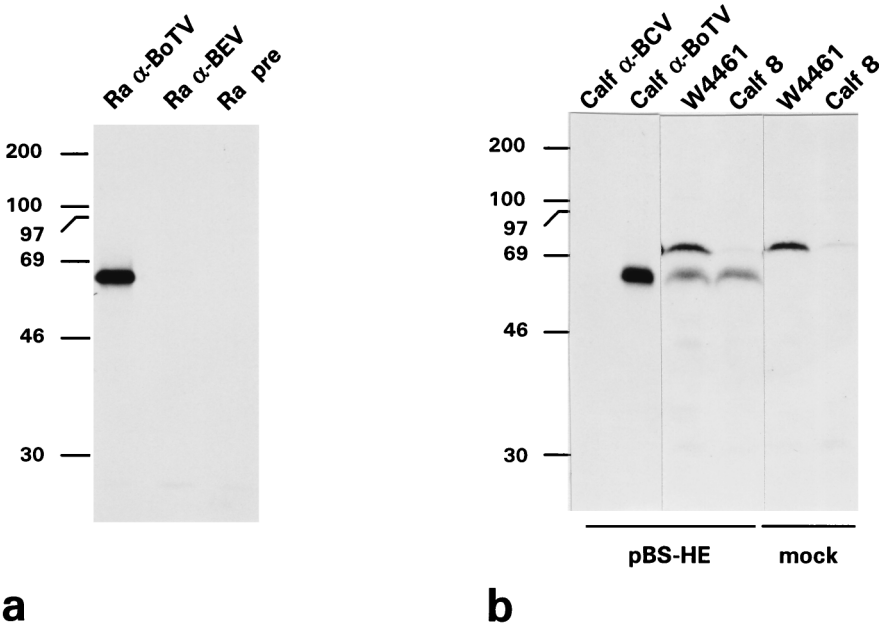

FIG. 4. Radioimmunoprecipitation of vTF7-3-expressed BoTV HE. (a) vTF7-3-infected cells were transfected with pBS-HE at 1 h p.i. and metabolically labeled from 5 to 6 h p.i. Cell lysates were subjected to immunoprecipitation (RIPA) with either rabbit antiserum raised against sucrose gradient-purified BoTV (Ra α-BoTV) or BEV (Ra α-BEV) or rabbit preimmune serum (Ra pre). (b) Detection of vTF7-3-expressed BoTV HE by antisera from BoTV-infected cattle. vTF7-3-infected cells were transfected or mock transfected with pBS-HE and metabolically labeled as described above. Cell lysates were subjected to RIPA with sera from an experimentally BoTV-infected gnotobiotic calf (serum GC76) (Calf α-BoTV), from a naturally infected cow (W4461), and from a sentinel calf (Calf 8) that acquired a BoTV infection upon exposure to adult seropositive cows (29). Serum from a gnotobiotic calf infected with bovine coronavirus (serum GC78) (Calf α-BCV) served as a negative control. The samples were analyzed in SDS–12.5% polyacrylamide gels. Molecular size markers (in kilodaltons) are indicated.

tated HE was analyzed by SDS-polyacrylamide gel electrophoresis (SDS-PAGE) under nonreducing conditions. The HE protein now migrated at 50K, its increased mobility indicating the presence of intrachain disulfide bonds. In contrast to coronavirus HE, vTF7-3-expressed BoTV HE did not readily form disulfide-linked oligomers (Fig. 5b). Products of 100K, possibly corresponding to HE dimers, were observed but only upon prolonged fluorography. These products remained EndoH sensitive, suggesting that they were retained in the ER (data not shown).

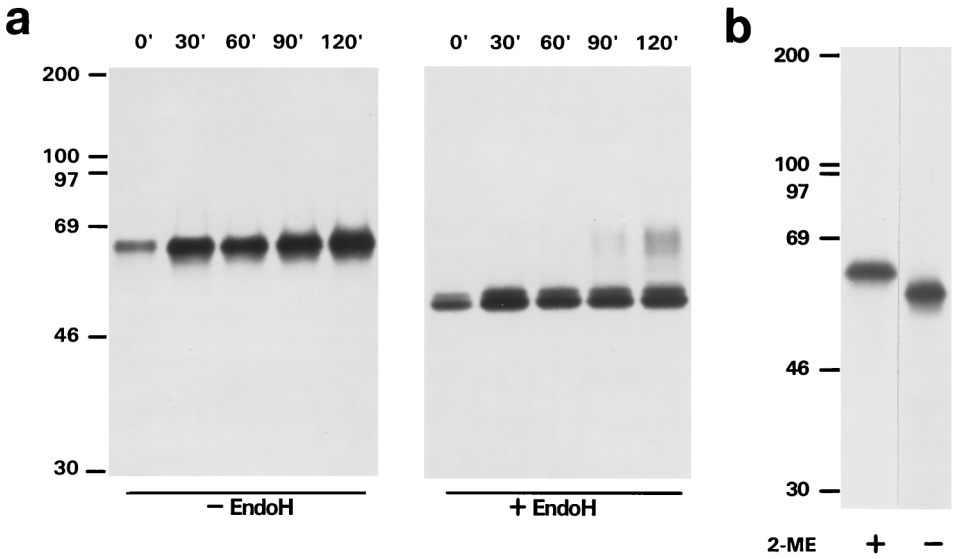

FIG. 5. Biosynthesis of BoTV HE in the vTF7-3 expression system. (a) Intracellular transport of BoTV HE. vTF7-3-infected, pBS-HE-transfected cells were metabolically labeled from 5 to 5.5 h p.i. and harvested either immediately (0 min) or after a chase for the indicated periods of time (in minutes). Cell lysates were subjected to RIPA with the rabbit anti-BoTV serum, and immunoprecipitated HE was treated with EndoH (+EndoH) or left untreated (−EndoH). The samples were analyzed under reducing conditions in an SDS-12.5% polyacrylamide gel. (b) Oligomerization of BoTV HE. vTF7-3-infected cells were transfected with pBS-HE and metabolically labeled from 5 to 5.5 h p.i. Cell lysates were prepared in the presence of 20 mM NEM. HE was immunoprecipitated with the rabbit anti-BoTV serum and analyzed under reducing conditions with 2-mercaptoethanol (2-ME) (+) or nonreducing conditions (−) in the same gel (SDS–10% PAGE). Molecular size markers (in kilodaltons) are indicated.

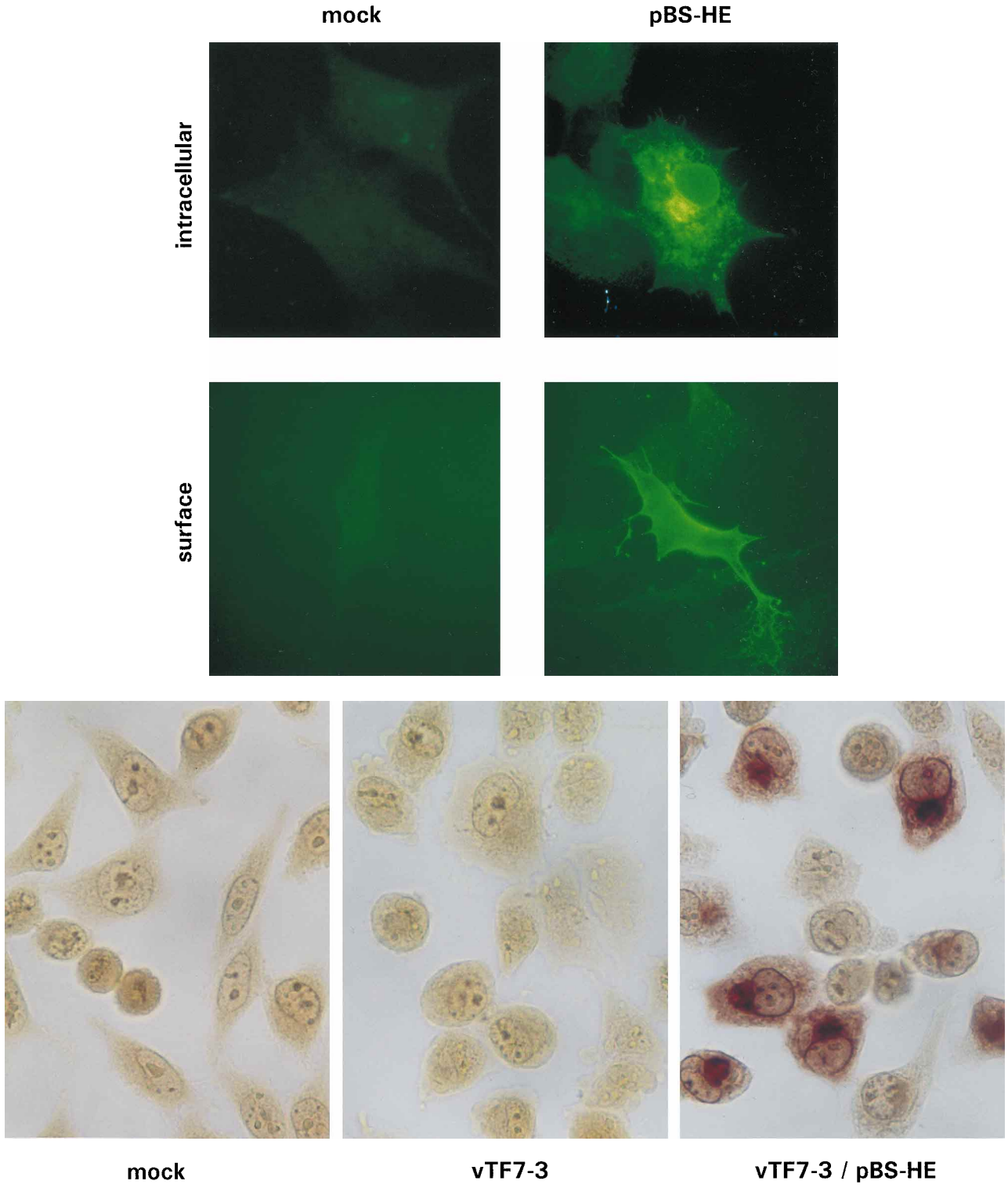

FIG. 6. (a) Detection of vTF7-3-expressed BoTV HE by immunofluorescence microscopy. BHK-21 cells grown on 12-mm-diameter gelatin-coated coverslips were infected with vTF7-3 and transfected with pBS-HE. At 6 h p.i. the cells were fixed with 3% paraformaldehyde and either permeabilized for internal immunofluorescence (upper panels) or left untreated (lower panels). Cells were stained for BoTV HE by using a rabbit anti-BoTV serum and fluorescein isothiocyanate-conjugated goat anti-rabbit immunoglobulin G. (b) BoTV HE displays acetylesterase activity. vTF7-3-infected, pBS-HE-transfected monolayers of OST7-1 cells were tested for acetylesterase activity by using α-naphthylacetate-pararosanilin as a substrate (63). Mock-infected and mock-transfected cells served as negative controls.

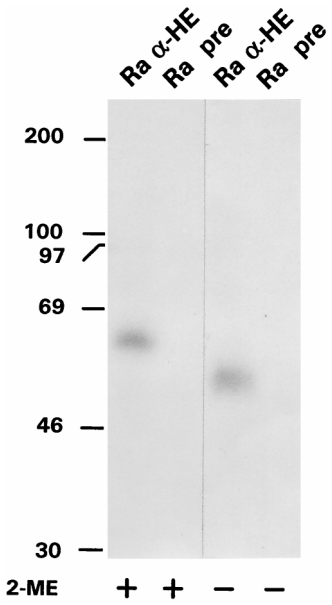

FIG. 7. Detection of the HE protein in radioiodinated BoTV preparations. BoTV, purified from fecal suspensions by pelleting through a 15% sucrose cushion followed by isokinetic sucrose gradient centrifugation (30), was radioiodinated with the Iodogen reagent as described previously (30). RIPA was performed with a rabbit antiserum raised against residues 13 to 130 of BoTV HE (Ra α-HE). Preimmune serum (Ra pre) served as a negative control. The immunoprecipitates were analyzed by SDS–10% PAGE under reducing conditions with 2-mercaptoethanol (2-ME) (+) or nonreducing conditions (−). Molecular size markers (in kilodaltons) are indicated.

Torovirus HE displays esterase activity. To determine whether BoTV HE possesses enzymatic activity, we employed an in situ esterase assay developed for ICV HEF (63). vTF7-3-infected OST7-1 cells were transfected with pBS-HE and at 6 h p.i. were tested for acetylesterase activity with α-naphthyl-acetate-pararosanilin as a substrate. Esterase activity, as demonstrated by widespread distribution of garnet-colored cells, was observed in pBS-HE-transfected monolayers but not in monolayers of mock-transfected or mock-infected cells (Fig. 6b). These results strongly suggest that the BoTV HE homolog is indeed an acetylesterase.

Torovirus HE is a structural protein. In the cases of ICV and coronavirus, the HE homologs are present in the viral envelope. To determine whether HE is also a structural protein of toroviruses, a rabbit antiserum was prepared against a bacterially expressed GST fusion protein containing residues 13 to 130 of HE. The antiserum, Ra α-HE, specifically detected vTF7-3-expressed BoTV HE in the RIPA and immunofluorescence assay (data not shown). BoTV, purified from feces by isokinetic sucrose gradient centrifugation, was exogenously labeled with ^{125}I as described previously (30) and, after lysis with 1% Triton-X100, subjected to RIPA. Upon SDS-PAGE analysis under reducing conditions, a 65K protein was detected with the Ra α-HE serum but not with the preimmune serum (Fig. 7). When analyzed under nonreducing conditions, this product migrated at 50K. Disulfide-linked oligomers were not observed (Fig. 7). These results suggested that HE was indeed a structural protein. However, to obtain formal evidence, we performed immunoelectron microscopy. As shown in Fig. 8, the Ra α-HE serum specifically bound to sucrose-gradient purified BoTV virions. Specific immunogold labeling of virions was not observed with rabbit preimmune serum or a rabbit antiserum directed against a GST fusion protein containing residues 255 to 328 of the feline herpesvirus gE protein (39). Close inspection of virions by electron microscopy revealed that in contrast to BEV (65, 66), BoTV contains two types of surface projections: in addition to the 17- to 20-nm petal-shaped peplomers, there was a second fringe of smaller spikes (6.3 ± 1 nm, n = 22) (Fig. 8a and data not shown). Presumably, these projections represent BoTV HE.

DISCUSSION

The HE homolog, a novel structural protein of torovirus. It has been postulated that the equine torovirus strain BEV is a deletion mutant that lost most of its HE gene (48), possibly during tissue culture adaptation. We now show that a field isolate of bovine torovirus contains an intact functional gene for an HE homolog. The bovine and equine torovirus isolates are closely related, having 84% nucleotide sequence identity in the 3′-most 3 kb of their genomes.

By using vTF7-3-expressed BoTV HE, antibodies were detected both in the convalescent-phase serum of a BoTV-infected gnotobiotic calf and in bovine field sera. Thus, the HE homolog is expressed during the natural infection and represents a prominent antigen. Immunoelectron microscopy studies identified the HE protein as a structural protein of torovirus. Close examination of electron micrographs of BoTV virions revealed, in addition to the large, 17- to 20-nm peplomers, the presence of shorter surface projections, 6 nm on average, closely resembling those formed by the HE proteins of coronaviruses (2, 56). Woode et al. (67) also described two types of surface projections for BoTV, but these authors considered the longer structures, i.e., the peplomers, to represent tissue debris. We postulate that the smaller surface projections, which are absent from the BEV virion (10, 65, 66), are composed of the BoTV HE homolog.

Expression of BoTV HE in the vTF7-3 expression system yielded a 65-kDa N-glycosylated protein. A product of this size was previously observed upon analysis of ^{125}I-labeled BoTV virions, but its virus specificity was not established (30). Here, we have unambiguously identified this protein as the HE homolog. A monospecific antiserum raised against HE specifically detected the 65-kDa protein in radioiodinated gradient-purified virus preparations. This finding strongly supports our conclusion that HE is part of the torovirus virion.

SDS-PAGE analysis of VTF7-3-expressed BoTV HE under nonreducing conditions showed that the protein does not readily assemble into disulfide-linked oligomeric complexes. Also, in the BoTV virion HE does not appear to form covalently linked oligomers. In contrast, the HE protein of coronavirus forms disulfide-linked homodimers (26, 44, 46) which are incorporated as such into the viral membrane (5, 12, 27, 28). Apparently, there are structural differences between the torovirus and coronavirus HE proteins. It is of note that the ICV HEF forms noncovalently linked homotrimers (20, 24). Most likely, the HE spikes of BoTV consist of noncovalently associated oligomeric structures. Whether these are di- or trimeric remains to be determined.

When expressed in cells, the BoTV HE protein was transported to the plasma membrane. However, as measured by the acquisition of EndoH resistance, this transport appeared to be slow. Toroviruses and coronaviruses both acquire their envelope by budding through intracellular membranes (15, 64), and intracellular retention of BoTV HE may well be an adaptation to ensure efficient incorporation into the virion. Alternatively, the slow transport of HE might be the result of its slow folding in the ER, as is the case with the coronavirus S protein (43).

Heterologous expression of BoTV HE also allowed us to

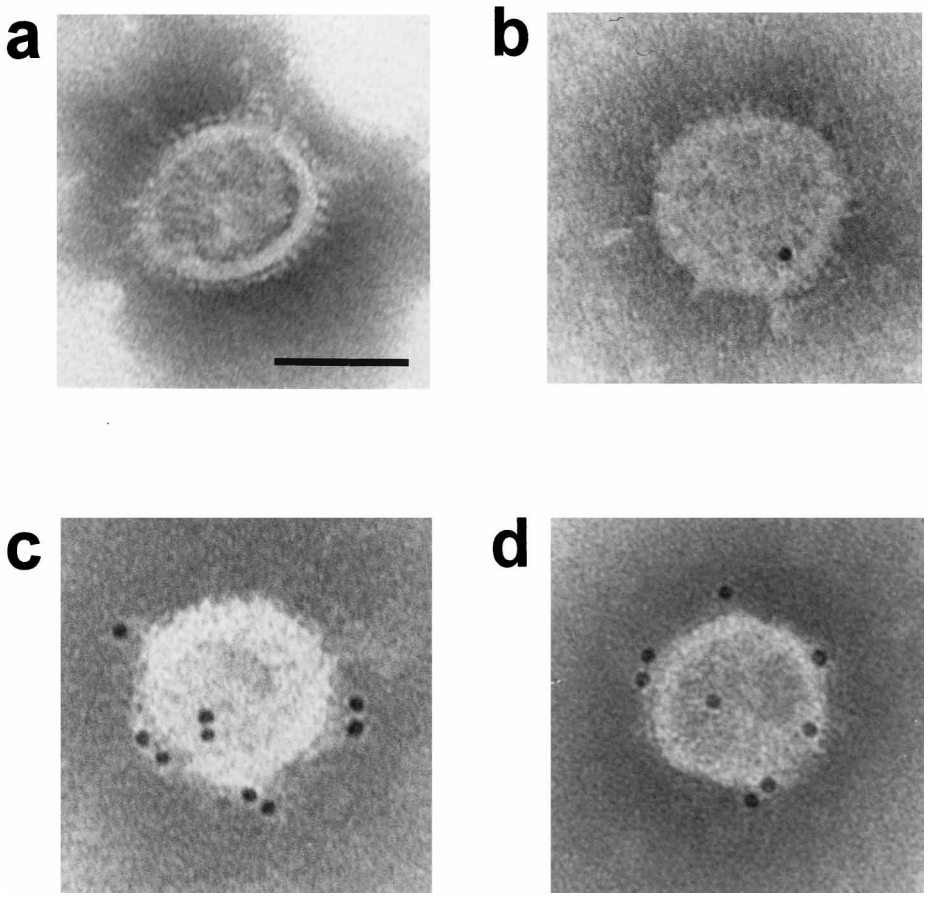

FIG. 8. Immunogold localization of the HE protein on the surface of BoTV virions by using the Ra α-HE serum and a protein A–5-nm colloidal gold conjugate. BoTV, purified by isokinetic and linear sucrose gradient centrifugation (30), was adsorbed to Formvar-carbon-coated copper grids. (a) General morphology of BoTV by negative staining with 2% sodium phosphotungstate, showing the presence of a fringe of 6-nm granular surface projections, which may represent BoTV HE. Specific immunogold labeling was obtained only with the Ra α-HE serum, raised against a bacterially expressed GST-HE fusion protein (c and d), and not with either rabbit preimmune serum (not shown) or a serum raised against an irrelevant GST expression product (b). Bar, 50 nm.

determine whether the protein is enzymatically active. Indeed, with α-naphthylacetate as a substrate in an in situ assay, esterase activity was specifically detected in vTF7-3-infected monolayers expressing HE. These results suggest that BoTV HE possesses an acetylesterase activity closely resembling that of ICV HEF and coronavirus HE.

The HE module, a host cell-derived sequence? The origin of the BoTV HE gene is unknown. Although corona- and toroviruses are related, they apparently acquired their HE genes through separate heterologous RNA recombination events. This is best illustrated by the fact that the HE genes are located at different positions in their genomes (48, 51) (Fig. 9). It is also of interest that the HE sequences of ICV, coronaviruses, and toroviruses are evolutionary equidistant and that several amino acid motifs, conserved in the HE(−1) of ICV and torovirus, have been lost in the coronavirus HE (Fig. 3). Vlasak et al. (58) proposed that the ICV HEF evolved from an ancestral gene related to the hemagglutinins (HAs) of influenza A and B viruses by subtle changes rather than through major gene rearrangements. However, a reevaluation of the results of Nakada et al. (41) and Pfeifer and Compans (45) showed that there is significant sequence similarity between the HA-2 and HE-2 subunits but not between the N-terminal regions of the HE-1 and HA-1 subunits (10). Thus, the ICV HEF may well have arisen by a heterologous recombination event in which the N-terminal part of the HA-1 subunit was replaced by an HE module. We would like to offer the hypothesis that ICV, coronaviruses, and toroviruses each have acquired the HE module independently from yet another source, perhaps by recombination with a host mRNA (Fig. 9). It is of note that a sialic acid-specific 9-*O*-acetylesterase, with an M_r of 65,000 and an enzymatic activity similar to that of ICV HEF, has been identified in rat liver cells (3, 4). However, recent sequence analysis suggests that this mammalian enzyme is not related to the viral acetylesterases (53).

In general, recombinant viruses will be lost from the viral population unless the acquired genetic information results in a gain of fitness. Apparently, the HE protein provides a considerable selective advantage, at least during the natural infection. The role of the ICV HEF in receptor binding and entry is well established (21, 55, 61), but the precise function of the HE proteins of corona- and toroviruses is still unknown. For coronaviruses, receptor binding and membrane fusion are mediated by the S protein (6). It has been suggested that the coronavirus HE may serve as an additional receptor-binding protein (44, 60). However, recent findings suggest that mouse hepatitis virus infection cannot be mediated by HE alone but requires the interaction of S with its receptor (17). Perhaps HE does not play a role in viral entry but plays a role at an even earlier step of the infection. ICV, coronaviruses, and torovi-

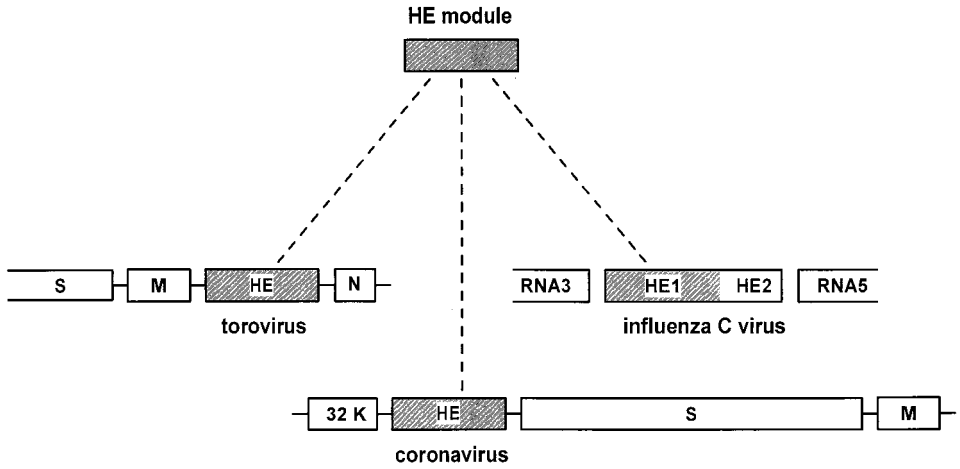

FIG. 9. Schematic model illustrating the capture of the HE module by ICV, coronavirus, and torovirus through heterologous recombination. The viral genomes are shown schematically. Boxes represent different genes (or genome segments, in the case of ICV). The HE module is indicated by a shaded box.

ruses infect the epithelial cells of the respiratory and enteric tracts. These cells are protected by a mucus layer, a gel formed by noncovalent interactions between large, highly hydrated glycoproteins, that can be up to 400 μm thick (for reviews, see references 38 and 40). This mucus layer thus presents a formidable barrier that has to be traversed before adsorption to the host cell can occur. The HE proteins may mediate viral adherence to the intestinal wall through the specific yet reversible binding to mucopolysaccharides. In fact, the process of binding to 9-*O*-acetylated receptors, followed by cleavage and rebinding to intact receptors, could theoretically even result in virus migration through the mucus layer and thereby facilitate not only the infection but also virus release and spread. Clearly, the role of the HE proteins during infection by corona- and toroviruses deserves further scrutiny.

ACKNOWLEDGMENTS

We thank G. Woode and B. Moss for providing antisera and virus stocks, J. Mol for help with the radioiodination experiments, and A. A. V. de Vries, J. W. A. Rossen, J. D. F. Mijnes, and J. M. V. M. Mouwen for stimulating discussions and helpful suggestions. We are grateful to P. J. M. Rottier for critically reading the manuscript, and we are indebted to W. F. Voorhout and A. Kroneman for advice and help with the immunoelectron microscopy experiments.

The research by R. J. de Groot was made possible by a fellowship from the Royal Netherlands Academy for Sciences and Arts.

REFERENCES

1. **Brian, D. A., B. G. Hogue, and T. E. Kienzle.** 1995. The coronavirus hemagglutinin esterase glycoprotein, p. 165–179. *In* S. G. Siddel (ed.), The Coronaviridae. Plenum Press, New York, N.Y.
2. **Bridger, J. C., E. O. Caul, and S. I. Egglestone.** 1978. Replication of an enteric bovine coronavirus in intestinal organ cultures. Arch. Virol. **57:**43–51.
3. **Butor, C., S. Diaz, and A. Varki.** 1993. High level O-acetylation of sialic acids on N-linked oligosaccharides of rat liver membranes. J. Biol. Chem. **268:** 10197–10206.
4. **Butor, C., H. H. Higa, and A. Varki.** 1993. Structural, immunological, and biosynthetic studies of a sialic acid-specific O-acetylesterase from rat liver. J. Biol. Chem. **268:**10207–10213.
5. **Callebaut, P. E., and M. B. Pensaert.** 1980. Characterization and isolation of structural polypeptides in haemagglutinating encephalomyelitis virus. J. Gen. Virol. **48:**193–204.
6. **Cavanagh, D.** 1995. The coronavirus surface glycoprotein, p. 73–113. *In* S. G. Siddel (ed.), The Coronaviridae. Plenum Press, New York, N.Y.
7. **Chao, L.** 1990. Fitness of RNA virus decreased by Muller's ratchet. Nature **348:**454–455.
8. **Chirnside, E. D., A. A. de Vries, J. A. Mumford, and P. J. Rottier.** 1995. Equine arteritis virus-neutralizing antibody in the horse is induced by a determinant on the large envelope glycoprotein G_L. J. Gen. Virol. **76:**1989–1998.
9. **Chreighton, T. E.** 1990. Protein structure: a practical approach. IRL Press, Oxford, United Kingdom.
10. **Cornelissen, L. A. H. M., and R. J. de Groot.** Unpublished data.
11. **Den Boon, J. A., E. J. Snijder, J. K. Locker, M. C. Horzinek, and P. J. Rottier.** 1991. Another triple-spanning envelope protein among intracellularly budding RNA viruses: the torovirus E protein. Virology **182:**655–663.
12. **Deregt, D., M. Sabara, and L. A. Babuik.** 1987. Structural proteins of bovine coronavirus and their intracellular processing. J. Gen. Virol. **68:**2863–2877.
13. **Eisenberg, D., E. Schwarz, M. Komaromy, and R. Wall.** 1984. Analysis of membrane and surface protein sequences with the hydrophobic moment plot. J. Mol. Biol. **179:**125–142.
14. **Elroy-Stein, O., and B. Moss.** 1990. Cytoplasmic expression system based on constitutive synthesis of bacteriophage T7 RNA polymerase in mammalian cells. Proc. Natl. Acad. Sci. USA **87:**6743–6747.
15. **Fagerland, J. A., J. F. L. Pohlenz, and G. N. Woode.** 1986. A morphological study of the replication of Breda virus (proposed family Toroviridae) in bovine intestinal cells. J. Gen. Virol. **67:**1293–1304.
16. **Fuerst, T. R., E. G. Niles, F. W. Studier, and B. Moss.** 1986. Eukaryotic transient-expression system based on recombinant vaccinia virus that synthesizes bacteriophage T7 RNA polymerase. Proc. Natl. Acad. Sci. USA **83:**8122–8126.
17. **Gagneten, S., O. Gout, M. Dubois-Dalcq, P. Rottier, J. Rossen, and K. V. Holmes.** 1995. Interaction of mouse hepatitis virus (MHV) spike glycoprotein with receptor glycoprotein MHVR is required for infection with an MHV strain that expresses the hemagglutinin-esterase glycoprotein. J. Virol. **69:**889–895.
18. **Goldbach, R., and J. Wellink.** 1988. Evolution of plus-strand RNA viruses. Intervirology **29:**260–267.
19. **Herrewegh, A. A. P. M., R. J. de Groot, A. Cepica, H. F. Egberink, M. C. Horzinek, and P. J. M. Rottier.** 1995. Detection of feline coronavirus RNA in feces, tissues, and body fluids of naturally infected cats by reverse transcriptase PCR. J. Clin. Microbiol. **33:**684–689.
20. **Herrler, G., A. Nagele, H. Meier-Ewert, A. S. Bhown, and R. W. Compans.** 1981. Isolation and structural analysis of influenza C virion glycoproteins. Virology **113:**439–451.
21. **Herrler, G., I. Durkop, H. Becht, and H.-D. Klenk.** 1988. The glycoprotein of influenza C virus is the haemagglutinin, esterase and fusion factor. J. Gen. Virol. **69:**839–846.
22. **Herrler, G., G. Multhaup, K. Beyreuther, and H.-D. Klenk.** 1988. Serine 71 of the glycoprotein HEF is located at the active site of the acetylesterase of influenza C virus. Arch. Virol. **102:**269–274.
23. **Herrler, G., R. Rott, H.-D. Klenk, H.-P. Muller, A. K. Shukla, and R. Schauer.** 1985. The receptor-destroying enzyme of influenza C virus is neuraminate O-acetylesterase. EMBO J. **4:**1503–1506.
24. **Hewat, E. A., S. Cusack, and R. W. H. Ruigrok.** 1984. Low resolution structure of the influenza C glycoprotein determined by electron microscopy. J. Mol. Biol. **175:**175–193.
25. **Hogue, B. G., T. E. Kienzle, and D. A. Brian.** 1989. Synthesis and processing of the bovine enteric coronavirus haemagglutinin protein. J. Gen. Virol. **70:**345–352.
26. **Kienzle, T. E., S. Abraham, B. G. Hogue, and D. A. Brian.** 1990. Structure

and orientation of expressed bovine coronavirus hemagglutinin-esterase protein. J. Virol. **64:**1834–1838.
27. **King, B., and D. A. Brian.** 1982. Bovine coronavirus structural proteins. J. Virol. **42:**700–707.
28. **King, B., B. J. Potts, and D. A. Brian.** 1985. Bovine coronavirus hemagglutinin protein. Virus Res. **2:**53–59.
29. **Koopmans, M., H. Cremers, G. N. Woode, and M. C. Horzinek.** 1990. Breda virus (Toroviridae) infection and systemic antibody response in sentinel calves. Am. J. Vet. Res. **51:**1443–1448.
30. **Koopmans, M., J. Ederveen, G. N. Woode, and M. C. Horzinek.** 1986. Surface proteins of Breda virus. Am. J. Vet. Res. **47:**1896–1900.
31. **Koopmans, M., and M. C. Horzinek.** 1995. The pathogenesis of torovirus infections in animals and humans, p. 403–413. *In* S. G. Siddel (ed.), The Coronaviridae. Plenum Press, New York, N.Y.
32. **Koopmans, M., U. Van den Boom, G. Woode, and M. C. Horzinek.** 1989. Seroepidemiology of Breda virus in cattle using ELISA. Vet. Microbiol. **19:**233–243.
33. **Krone, W. J. A., C. Debouk, L. G. Epstein, P. Heutink, R. Meloen, and J. Goudsmit.** 1988. Natural antibodies to HIV-tat epitopes and expression of HIV-1 gene in vivo. J. Med. Virol. **26:**261–270.
34. **Lai, M. M.** 1992. Genetic recombination in RNA viruses. Curr. Top. Microbiol. Immunol. **176:**21–32.
35. **Luytjes, W.** 1995. Coronavirus gene expression; genome organization and protein synthesis, p. 33–54. *In* S. G. Siddel (ed.), The Coronaviridae. Plenum Press, New York, N.Y.
36. **Luytjes, W., P. Bredenbeek, A. Noten, M. C. Horzinek, and W. Spaan.** 1988. Sequence of mouse hepatitis virus A59 mRNA2: indications for RNA recombination between coronaviruses and influenza C virus. Virology **166:**415–422.
37. **Machamer, C. E., S. A. Mentone, J. K. Rose, and M. G. Farquhar.** 1990. The E1 glycoprotein of an avian coronavirus is targeted to the cis Golgi complex. Proc. Natl. Acad. Sci. USA **87:**6944–6948.
38. **Mantle, M., and A. Allen.** 1989. Gastrointestinal mucus, p. 202–229. *In* J. S. Davidson (ed.), Gastrointestinal secretion. Butterworth and Co., Ltd., London, United Kingdom.
39. **Mijnes, J. D. F., L. M. Van der Horst, E. Van Anken, M. C. Horzinek, P. J. M. Rottier, and R. J. de Groot.** 1996. The biosynthesis of glycoproteins E and I of feline herpesvirus: gE-gI interaction is required for intracellular transport. J. Virol. **70:**5466–5475.
40. **Mouwen, J. M. V. M., H. J. A. Egberts, and J. F. J. G. Koninkx.** 1983. The outermost mucosal barrier of the mammalian small intestine. Dtsch. Tieraerztl. Wochenschr. **90:**459–502.
41. **Nakada, S., R. S. Creager, M. Krystal, R. P. Aaronson, and P. Palese.** 1984. Influenza C virus hemagglutinin: comparison with influenza A and B virus hemagglutinins. J. Virol. **50:**118–124.
42. **Neuberger, A., A. Gottschalk, R. O. Marshall, and R. G. Spiro.** 1972. Carbohydrate-peptide linkages in glycoproteins and methods for their elucidation, p. 450–490. *In* A. Gottschalk (ed.), The glycoproteins: their composition, structure and function. Elsevier, Amsterdam, The Netherlands.
43. **Opstelten, D.-J., P. De Groote, M. C. Horzinek, H. Vennema, and P. J. M. Rottier.** 1993. Disulfide bonds in folding and transport of mouse hepatitis coronavirus glycoproteins. J. Virol. **67:**7394–7401.
44. **Parker, M. D., G. J. Cox, D. Deregt, D. R. Fitzpatrick, and L. A. Babuik.** 1989. Cloning and in vitro expression of the gene for the E3 haemagglutinin glycoprotein of bovine coronavirus. J. Gen. Virol. **70:**155–164.
45. **Pfeifer, J. B., and R. W. Compans.** 1984. Structure of the influenza C glycoprotein gene as determined from cloned DNA. Virus Res. **1:**281–296.
46. **Pfleiderer, M., E. Routledge, G. Herrler, and S. G. Siddell.** 1991. High level transient expression of the murine coronavirus haemagglutinin-esterase. J. Gen. Virol. **72:**1309–1315.
47. **Smith, D. B., M. R. Rubira, R. J. Simpson, K. M. Davern, W. U. Tiu, P. G. Board, and G. F. Mitchell.** 1988. Expression of an enzymatically active parasite molecule in E. coli: Schistosoma japonicum glutathione-S-transferase. Mol. Biochem. Parasitol. **98:**503–516.
48. **Snijder, E. J., J. A. den Boon, M. C. Horzinek, and W. J. Spaan.** 1991. Comparison of the genome organization of toro- and coronaviruses: evidence for two nonhomologous RNA recombination events during Berne virus evolution. Virology **180:**448–452.
49. **Snijder, E. J., J. A. Den Boon, W. J. Spaan, M. Weiss, and M. C. Horzinek.** 1990. Primary structure and post-translational processing of the Berne virus peplomer protein. Virology **178:**355–363.
50. **Snijder, E. J., J. A. den Boon, W. J. M. Spaan, G. M. G. M. Verjans, and M. C. Horzinek.** 1989. Identification and primary structure of the gene encoding the Berne virus nucleocapsid protein. J. Gen. Virol. **70:**3363–3370.
51. **Snijder, E. J., and M. C. Horzinek.** 1995. The molecular biology of torovirus, p. 219–238. *In* S. G. Siddel (ed.), The Coronaviridae. Plenum Press, New York, N.Y.
52. **Snijder, E. J., M. C. Horzinek, and W. J. Spaan.** 1990. A 3′-coterminal nested set of independently transcribed mRNAs is generated during Berne virus replication. J. Virol. **64:**331–338.
53. **Stoddart, A., Y. Zhang, and C. J. Paige.** 1996. Molecular cloning of the cDNA encoding a murine sialic acid-specific 9-*O*-acetylesterase and RNA expression in cells of hematopoietic and non-hematopoietic origin. Nucleic Acids Res. **24:**4003–4008.
54. **Strauss, J. H., and E. G. Strauss.** 1988. Evolution of RNA viruses. Annu. Rev. Microbiol. **42:**657–683.
55. **Strobl, B., and R. Vlasak.** 1993. The receptor-destroying enzyme of influenza C virus is required for entry into target cells. Virology **192:**679–682.
56. **Sugiyama, K., and Y. Amano.** 1981. Morphological and biological properties of a new coronavirus associated with diarrhea in infant mice. Arch. Virol. **67:**241–251.
57. **Vennema, H., G.-J. Godeke, J. W. A. Rossen, W. F. Voorhout, M. C. Horzinek, D.-J. Opstelten, and P. J. M. Rottier.** 1996. Nucleocapsid-independent assembly of coronavirus-like particles by co-expression of viral envelope protein genes. EMBO J. **15:**2020–2028.
58. **Vlasak, R., M. Krystal, M. Nacht, and P. Palese.** 1987. The influenza C virus glycoprotein (HE) exhibits receptor-binding (hemagglutinin) and receptor-destroying (esterase) activities. Virology **160:**419–425.
59. **Vlasak, R., W. Luytjes, J. Leider, W. Spaan, and P. Palese.** 1988. The E3 protein of bovine coronavirus is a receptor-destroying enzyme with acetyl esterase activity. J. Virol. **62:**4686–4690.
60. **Vlasak, R., W. Luytjes, W. Spaan, and P. Palese.** 1988. Human and bovine coronaviruses recognize sialic acid containing receptors similar to those of influenza C viruses. Proc. Natl. Acad. Sci. USA **85:**4526–4529.
61. **Vlasak, R., T. Muster, A. M. Lauro, J. C. Powers, and P. Palese.** 1989. Influenza C virus esterase: analysis of catalytic site, inhibition, and possible function. J. Virol. **63:**2056–2062.
62. **Von Heijne, G.** 1986. A new method for predicting signal sequence cleavage sites. Nucleic Acids Res. **14:**4683–4690.
63. **Wagaman, P. C., H. A. Spence, and R. J. O'Callaghan.** 1989. Detection of influenza C virus by using an in situ esterase assay. J. Clin. Microbiol. **27:**832–836.
64. **Weiss, M., and M. C. Horzinek.** 1986. Morphogenesis of Berne virus (proposed family Toroviridae). J. Gen. Virol. **67:**1305–1314.
65. **Weiss, M., and M. C. Horzinek.** 1987. The proposed family Toroviridae: agents of enteric infections. Arch. Virol. **92:**1–15.
66. **Weiss, M., F. Steck, and M. C. Horzinek.** 1983. Purification and partial characterization of a new enveloped RNA virus (Berne virus). J. Gen. Virol. **64:**1849–1858.
67. **Woode, G. N., D. E. Reed, P. L. Runnels, M. A. Herrig, and H. T. Hill.** 1982. Studies with an unclassified virus isolated from diarrhoeic calves. Vet. Microbiol. **7:**221–240.
68. **Woode, G. N., L. J. Saif, M. Quesada, N. J. Winand, J. F. Pohlenz, and N. Kelso Gourley.** 1985. Comparative studies on three isolates of Breda virus of calves. Am. J. Vet. Res. **46:**1003–1010.
69. **Zimmern, D.** 1987. Evolution of RNA viruses, p. 211–240. *In* J. J. Holland, E. Domingo, and P. Ahlquist (ed.), RNA genetics, vol. 2. CRC Press, Boca Raton, Fla.